17èmes Journées Internationales de Thermique (JITH 2015)
Marseille (France), 28 - 30 Octobre 2015

Turbulent Flow and Heat Transfer of Water-Al_2O_3 Nanofluid in Horizontal Corrugated Channel

Rachid BOUCHENAFA[1,2], Rachid SAIM[1], Said ABBOUDI[2]
(1) Laboratoire Energétique et Thermique Appliquée (ETAP)
Faculté de technologie, Université de Tlemcen BP 230, Algérie Adresse des auteurs
(2) IRTES-M3M - EA 7274, Université de Technologie de Belfort-Montbéliard site de Sévenans, 90010 Belfort cedex, France
bouchenafa_rachid2011@yahoo.com *saimrachid@yahoo.fr* *s.abboudi@utbm.fr*

Abstract: This investigation aims to study numerically turbulent flow and heat transfer of water-Al2O3 Nanofluid in horizontal corrugated channel. The governing equations (continuity, momentum and energy) fitted with boundary conditions are solved by the finite volume method and the SIMPLE algorithm for velocity pressure coupling. The k-ε standard model is chosen for modeling the turbulence. The effect of four different corrugation shapes (α=0°, 20°, 30°and 45°) and four different volumes fractions (Φ =1%, 2%, 3% and 4%) of Nanofluid are examined. The upper and lower walls of channel are maintained at a constant temperature, and the Reynolds number range from 5,000 to 20,000. The results show that using the corrugated walls and the Nanofluid improve significantly the thermal-hydraulic performances.

Key words: corrugated channel, nanofluid, turbulent, heat transfer, finite volume

1. Introduction

The enhancement of hydrodynamic and heat transfer characteristics in grooved channels by using the Nanofluid represents a subject of interest for several engineering applications, such as in heat exchangers, medical, refrigerators, automobiles and electronics cooling. Many research works were performed to study the flow and convection heat transfer in various corrugated channels. He et al. [1] numerically studied convective heat transfer of TiO_2 nanofluids flowing through a straight tube under the laminar flow conditions. The results showed significant enhancement of heat transfer of nanofluids particularly in the entrance region. The effects of using various types of nanofluids and the Reynolds numbers on heat transfer and fluid flow characteristics in a square shaped microchannel heat exchanger was investigated by Mohammed et al [2]. An experimental study on converging–diverging tubes turbulent flow in the entrance and fully developed regions was performed by Mendes and Sparrow [3]. They investigated the effect of different aspect ratios and taper angles on the heat and mass transfer behaviors. The results showed an overall enhancement in heat transfer rates for the converging–diverging channel compared with the straight tubes. Sang and Hyung [4] conducted experimental and numerical study on flow and local heat and mass transfer characteristics of wavy duct using a naphthalene sublimation technique. The flow visualization and CFD simulation were used to predict the overall flow structures inside the duct. The results showed that complex secondary flows and transfer processes exist inside the wavy duct resulting in non-uniform distributions of the heat and mass transfer coefficients on the duct side walls. They reported that the average heat/mass transfer coefficients are higher than those of the smooth circular duct, and. that enhancement was accompanied by increased pressure drop penalty. Pingan et al. [5] employed standard k–ε turbulence model and enhanced wall treatment to investigate the air flow-field, heat transfer and resistance coefficient in two-dimensional channels with different ribs shapes. The average Nusselt number of the channel heated wall with triangular ribs was the largest, and was smallest in the channel with rectangular ribs. The resistance coefficient of the channel heated wall with triangular ribs was the largest, and was the smallest in the channel with semicircular ribs. Qu et al. [6] performed an experimental and numerical study through trapezoidal silicon microchannels with hydraulic diameters from 62 mm to 169 mm. Comparative results indicated that the Nusselt number obtained by experimental methods is markedly lower than that obtained by numerical analysis. The effects of three different types of nanofluid on thermophysical properties and heat transfer characteristics of a plate heat exchanger were analyzed by Javadi et al [7]. The effect of triangular roughness on laminar convective heat transfer in two dimensional parallel plate microchannels with constant wall temperature was studied numerically by Turgay and Yazicioglu [8]. In their study, the slip velocity and temperature jump at wall boundaries were considered to have a rare faction effect. The results showed that increasing surface roughness reduces heat transfer in continuum while an increase in the Nusselt number with increasing roughness height was observed in slip flow regime. Xuan and Li [9] experimentally investigated the convective heat transfer feature

and flow performance of copper–water nanofluid in a tube. It was found that the suspended nanoparticles remarkably improve heat transfer performance of the base fluid. Compared to water at the same value of Reynolds number, the Nusselt number in the nanofluid case was increased by more than 39% for nanofluid containing 2.0% volume fraction of copper nanoparticles. Santra et al. [10] numerically studied the heat transfer behavior of copper–water nanofluid in a two dimensional horizontal duct. The governing equations for laminar flow were discretized using finite volume approach and solved iteratively using the SIMPLER algorithm. It was observed that the rate of heat transfer increases with the increase in the flow rate and Nanoparticle volume fraction. Abed et al. [11] presented a numerical study of the heat transfer and flow characteristics in corrugated with V-shape lower plate using nanofluids. The computations are performed uniform heat flux over a range of Reynolds number (Re) 8000–20,000. They found that these V-shaped wavy channels have advantages by using nanofluids and thus serve as promising candidates for incorporation into efficient heat transfer devices. Akbarinia and Laur [12] numerically investigated the effect of nanoparticle on laminar mixed convection heat transfer in a circular curved tube with a nanofluid consisting of water and Al_2O_3-water Nanofluid (1%). It was found that increasing the diameter of the nanoparticle decreases the Nusselt number and secondary flow, while the axial velocity augments. The laminar forced convection of Cu-water nanofluid in a partially heated microchannel was investigated by Raisi et al. [13]. The effects of both slip and no-slip boundary conditions on the flow field and heat transfer were considered in their study. It was observed that the solid volume fraction as well as slip velocity coefficient has been great effects on heat transfer rate especially at high Reynolds numbers.

The main objective of the present numerical study is to examine the effect of four triangular different corrugation shapes (α=0°, 20°, 30°and 45°), and four different volumes fractions (Φ =1%, 2%, 3% and 4%) on the thermal and hydraulic performances of Al_2O_3 Nanofluid in horizontal channel.

2. Problem definition and mathematical model

2.1 Geometry of the problem

The geometry studied is shown in Figure 1. It consists of a horizontal channel with length L, height H, and provided with a triangular cavities. The inlet and the outlet of the channel are extended by L_i and L_0 respectively. The pitch P between two successive cavities is kept constant. Each cavity has a length w and height e, the inclination α takes four values. The geometrical parameters are summarized in Table 1.

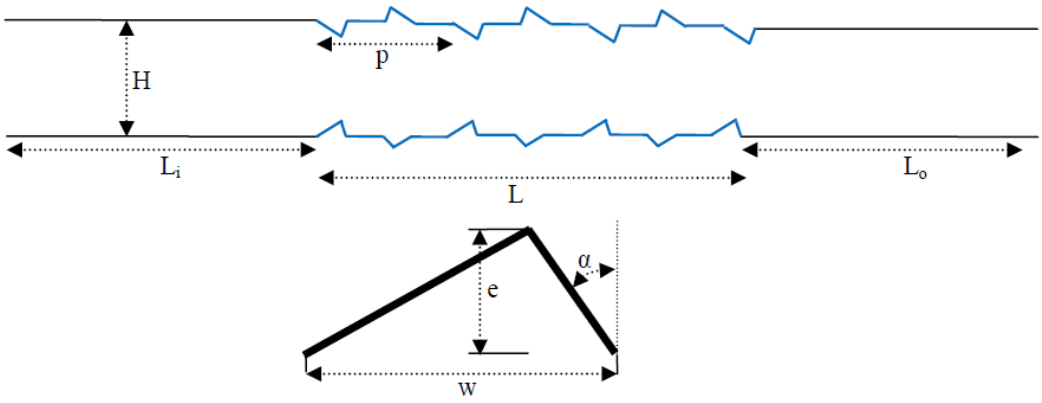

Figure 1: Schematic diagram of the channel

Table 1 Geometrical parameters

L *(mm)*	L_i *(mm)*	L_0 *(mm)*	H *(mm)*	P *(mm)*	w *(mm)*	e *(mm)*	α *(°)*
110	200	30	10	24	2	1	0 20 30 45

2.2 Governing equations:

The phenomenon under consideration is governed by the steady two-dimensional form of the continuity, the averaged incompressible Navier–Stokes equations and energy equation. In the Cartesian tensor system, these equations can be written as [14]:

2.2.1Continuity equation:

$$\frac{\partial}{\partial x_i}(\rho u_i) = 0 \tag{1}$$

2.2.2Momentum equation:

$$\frac{\partial(\rho u_i u_j)}{\partial x_i} = -\frac{\partial P}{\partial x_i} + \frac{\partial}{\partial x_j}\left[\mu\left(\frac{\partial u_i}{\partial x_j} + \frac{\partial u_j}{\partial x_i}\right)\right] + \frac{\partial}{\partial x_j}(-\rho\overline{u'_i u'_j}) \tag{2}$$

2.2.3 Energy equation:

$$\frac{\partial}{\partial x_i}(\rho u_i T) = \frac{\partial}{\partial x_j}\left((\Gamma + \Gamma_t)\frac{\partial T}{\partial x_j}\right) \tag{3}$$

Where Γ and Γ_t are molecular thermal diffusivity and turbulent thermal diffusivity, respectively and are given by:

$$\Gamma = \frac{\mu}{\Pr} \quad \text{And} \quad \Gamma_t = \frac{\mu_t}{\Pr_t} \tag{4}$$

Reynolds stresses $(-\rho\overline{u'_i u'_j})$ in Eq. (2) is modelled by equation (5).

$$-\rho\overline{u'_i u'_j} = \mu_t\left(\frac{\partial u_i}{\partial x_j} + \frac{\partial u_j}{\partial x_i}\right) \tag{5}$$

The turbulent viscosity term μ_t is to be computed from an appropriate turbulence model. The expression for the turbulent viscosity is given as:

$$\mu_t = \rho C_\mu \frac{k^2}{\varepsilon} \tag{6}$$

The modeled equation of the turbulent kinetic energy (k) is written as:

$$\frac{\partial}{\partial x_i}(\rho k u_i) = \frac{\partial}{\partial x_j}\left[\left(\mu_t + \frac{\mu_t}{\sigma_t}\right)\frac{\partial k}{\partial x_j}\right] + G_k - \rho\varepsilon \tag{7}$$

Similarly the turbulence dissipation rate ε is given by the following equation:

$$\frac{\partial}{\partial x_i}(\rho\varepsilon u_i) = \frac{\partial}{\partial x_j}\left[\left(\mu + \frac{\mu_t}{\sigma_k}\right)\frac{\partial \varepsilon}{\partial x_j}\right] + C_1\frac{\varepsilon}{k}G_k - C_{2\varepsilon}\rho\frac{\varepsilon^2}{k} \tag{8}$$

Where G_k is the rate of generation of the TKE while ρ ε is its destruction rate. G_k is written as:

$$G_k = -\rho\overline{u'_i u'_j}\frac{\partial u_j}{\partial x_i} \tag{9}$$

The empirical constants for the turbulence model are arrived by comprehensive data fitting for a wide range of turbulent flow:

C_μ=0.09, $C_{\varepsilon 1}$=1.47, $C_{\varepsilon 2}$=1.92, σ_k=1.0, σ_ε=1.3

2.3 Boundary conditions:

The boundary conditions of this study are presented in Figure 2. The upper and lower corrugated walls of the channel are maintained at a constant temperature T_w, and the extended walls are adiabatic. At the inlet, the fluid enters the channel with a uniform velocity and uniform temperature. At the outlet, the flow may safely be assumed as fully-developed, which implies negligible stream wise gradients of all variables.

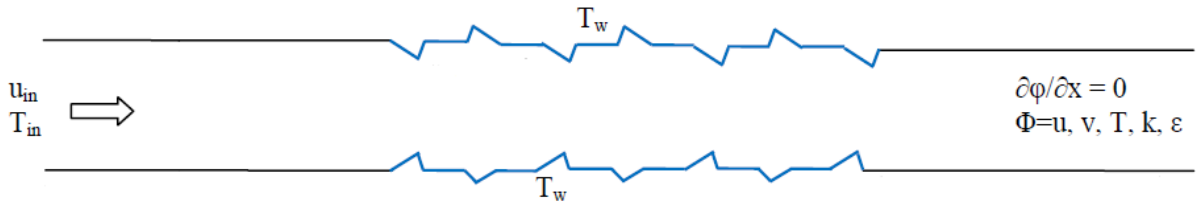

Figure 2**:** Boundary conditions.

2.4 Thermophysical properties of fluid and nanofluids [15]:

The thermophysical properties of nanofluids used in this study were obtained using the following equations: The density of Nanofluid ρ_{nf} obtained from the following equation:

$$\rho_{nf} = (1-\phi)\rho_f + \phi\rho_{np} \tag{11}$$

Where ρ_f and ρ_{np} are the mass densities of the base fluid and the solid nanoparticles, respectively.
The effective heat capacity at constant pressure of Nanofluid can be calculated from the following equation

$$(\rho C_p)_{nf} = (1-\phi)(\rho C_p)_f + \phi(\rho C_p)_{np} \tag{12}$$

Where $(\rho C_p)_f$ and $(\rho C_p)_{np}$ are heat capacities of the base fluid and the solid nanoparticles, respectively.
The effective thermal conductivity can be obtained by using the following mean empirical correlation:

$$k_{eff} = k_{static} + k_{Brownian} \tag{13}$$

$$k_{static} = k_f \left[\frac{(k_{np} + 2k_f) - 2\phi(k_f - k_{np})}{(k_{np} + 2k_f) + \phi(k_f + k_{np})} \right] \tag{14}$$

$$k_{Brownian} = 5*10^4 \beta\phi\rho_f Cp_f \sqrt{\frac{KT}{2\rho_{np}R_{np}}} f(T,\phi) \tag{15}$$

Where K is the Boltzmann constant, K= $1.3807*10^{-23}$ J/K
The values of β for different particles are listed in Table 2

Table 2 Curve-fit relations proposed by Vajjha and Das [16]

particles	β	Concentration (%)	Temperature (K)
Al_2O_3	8.4407 (100 Φ) -1.07304	1% ≤ Φ ≤10%	298 ≤ T ≤ 363

$$f(T,\phi) = (2.8217*10^{-2}\phi + 3.917*10^{-3})\left(\frac{T}{T_0}\right) + (-3.0669*10^{-2}\phi - 3.391123*10^{-23}) \tag{16}$$

For 1% ≤ Φ≤ 4% and 300K < T <325K
The effective viscosity can be obtained by using the following mean empirical correlation:

$$\mu_{eff} = \mu_f * \frac{1}{(1 - 34.87(dp/df)^{-0.3} * \phi 10^{-3})} \tag{17.a}$$

$$df = \left[\frac{6M}{N\pi\rho_{f0}} \right]^{1/3} \tag{17.b}$$

The thermophysical properties of nanoparticle and base fluid are mentioned in Table 2.

Table 2. Thermophysical properties of nanoparticle and base fluid at T=300 K.

Thermophysical properties	Al_2O_3	water
ρ (kg/m^3)	3600	996.5
Cp (J/kg K)	765	4181
k (W/m K)	36	0.613
μ (Ns/m2)	-	1E-03

The Reynolds number, the Nusselt number, and the friction factor are given by the following relations:

$$\mathrm{Re} = \frac{\rho u_{in} D_h}{\mu} \tag{18}$$

$$Nu = \frac{hD_h}{k} \tag{19}$$

$$f = 2\Delta P \frac{D_h}{\rho L u_{in}^2} \tag{20}$$

3. Results and discussion

3.1 Grid independence and code validation:

To check for the independence of the results from the number of grid points used, a serial of test simulation in the computational domain corresponds to the velocity inlet equal to 0.753 m/s (Re=15.000). A uniform quadratic mesh, with a refinement near the upper and lower walls, is used for all simulations in this study due the

uniform geometries. The grid independence test is conducted by assuming different grid distributions of 79.576, 88.276 and 104485. As shown in figure 3, the axial velocity profiles at the position x=0.2 m present a small variation which is considered a criterion for grid independence.

To verify the computational model and the method adopted in current numerical simulation, the numerical study was validated with experimental and numerical results obtained by Eiamsa [17]. Figure 4 presents the variation of average Nusselt number with Reynolds number. It is clear that the results are exhibited good agreement which allowed us to study the problem numerically.

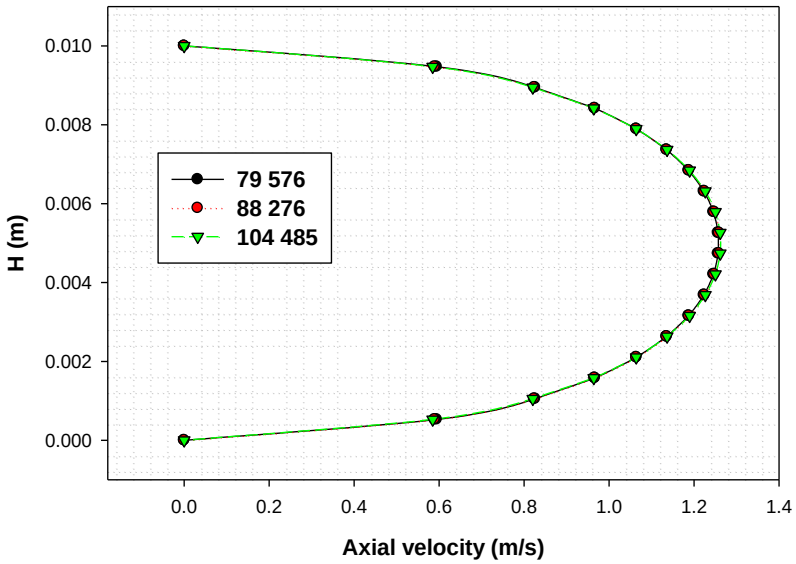

Figure 3 Effect of grid on axial velocity

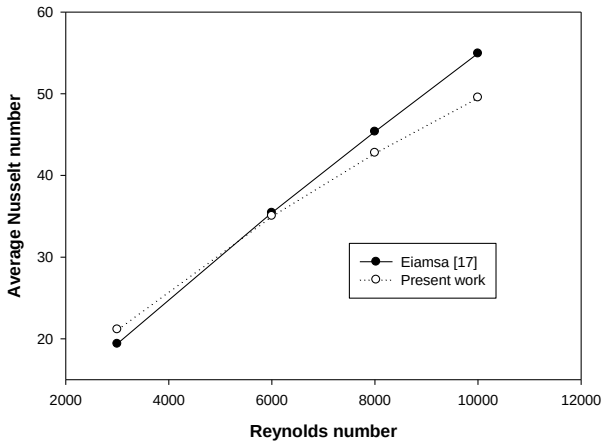

Figure 4 Comparison of our results in terms of average Nusselt number with those of experimental

3.3 Effect of the angle α

The impact of the angle α on the flow structure is presented in Figure 5 where the inlet velocity correspond a Reynolds number Re=10.000, and the concentration of nanoparticle is Φ = 2 %. The first and the second triangular corrugations are choosen to present the velocity contours. As seen from the figure, a vortex (recirculation zones) is generated behind the first corrugation. In the in the channel center, the axial velocity increases by increasing the inclination α.

Figure 5 velocity contours

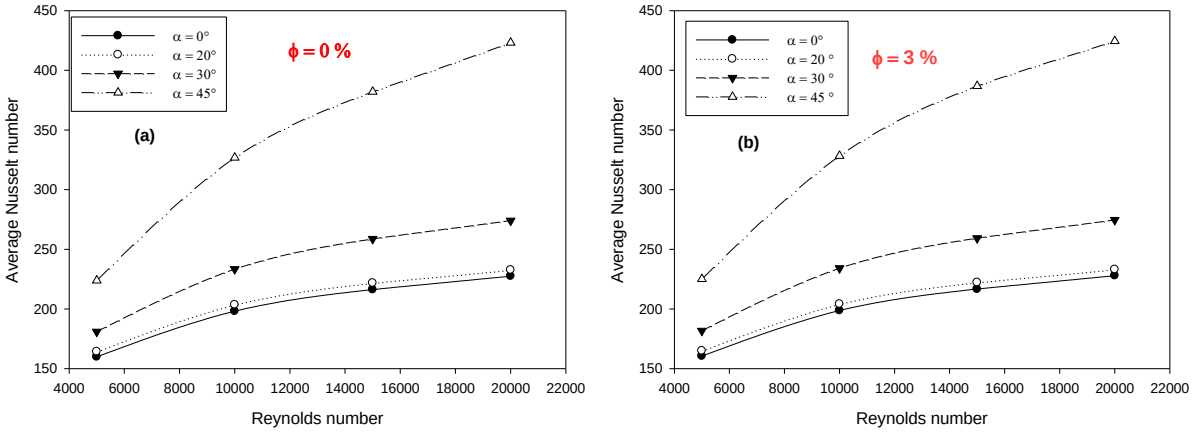

Figure 6 Average Nusselt number, a) Φ=0%, b) Φ=3%

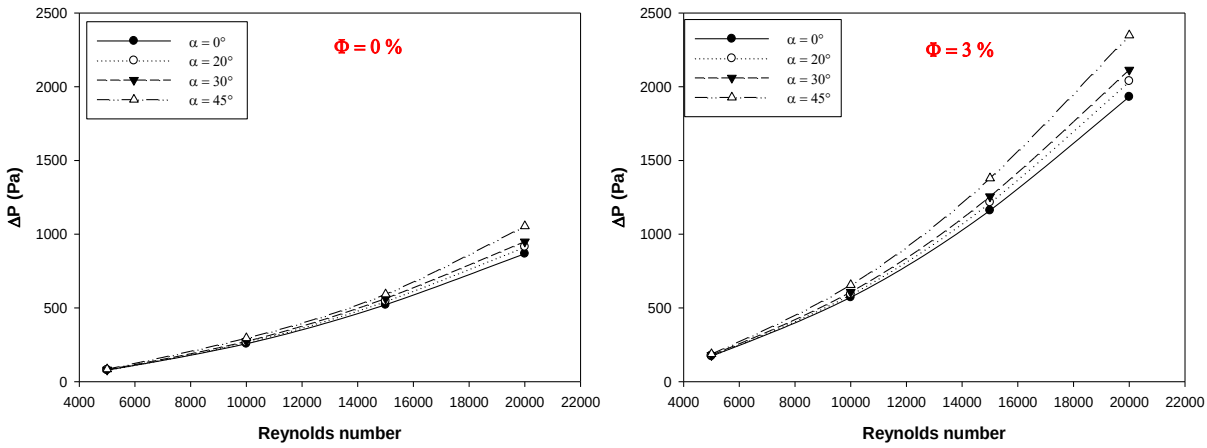

Figure 7 Pressure drop, a) Φ=0%, b) Φ=3%

The figures 6(a) and 6(b) present the average Nusselt number as function of Reynolds number for two concentration nanoparticles 0% and 3% respectively. It is clear that the average Nusselt number increases by increasing the angle α and the Reynolds number. For both cases, the triangular shape with α=45° have the highest value of average Nusselt number compared with the other cases. This growth in Nusselt number can be explained by the strong turbulence intensity of the presence of the corrugation leading to rapid mixing between the nanofluid and the walls of channel.

The pressure drop as function of Reynolds number for four angles and for pure water (Φ=0%) and volume fraction Φ=3% is presented on figures 7 (a) and 7 (b) respectively. For the both cases, the pressure drop increases by increasing Reynolds number and the inclination α. As shown in figures, the use of nanofluid causes more pressure drop and this due to the increase in viscosity.

3.4 Effect of volume fraction

In this investigation, the nanoparticle volume fraction range of 1% to 4%. Figures 8 (a) and 8 (b) show the effect of nanoparticle volume fraction as function of Reynolds number for two cases α=0° and α=45° respectively. By increasing the Reynolds number, the average Nusselt number increases and this can be explained by the increase of the movements of nanoparticles which increase the energy rates in the fluid. By increasing the volume fraction of the nanofluid, the thermal conductivity of the water increases and therefore the heat transfer enhanced.

Figures 9 (a) and 9 (b) present the pressure drop as function of Reynolds number for all volume fraction (1% to 4%) and for two inclinations α = 0° and α = 45° respectively. It is clear that the pressure drop increases by increasing Reynolds number for pure water and nanofluids. The pressure drop increases also with volume fraction increasing due to increasing in density and viscosity. For height Reynolds number, the rate of pressure drop is more important compared with low Reynolds number.

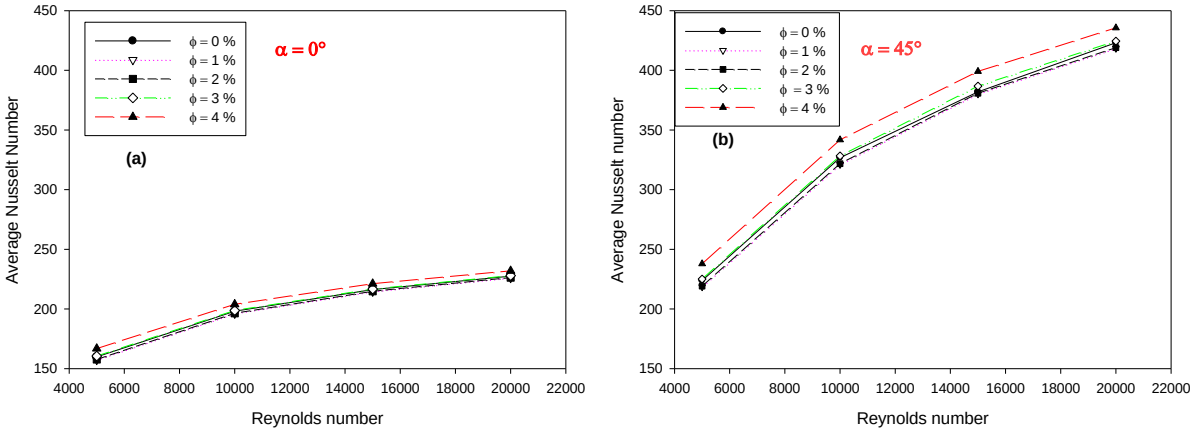

Figure 8 Average Nusselt number, a) α=0°, b) α = 45°

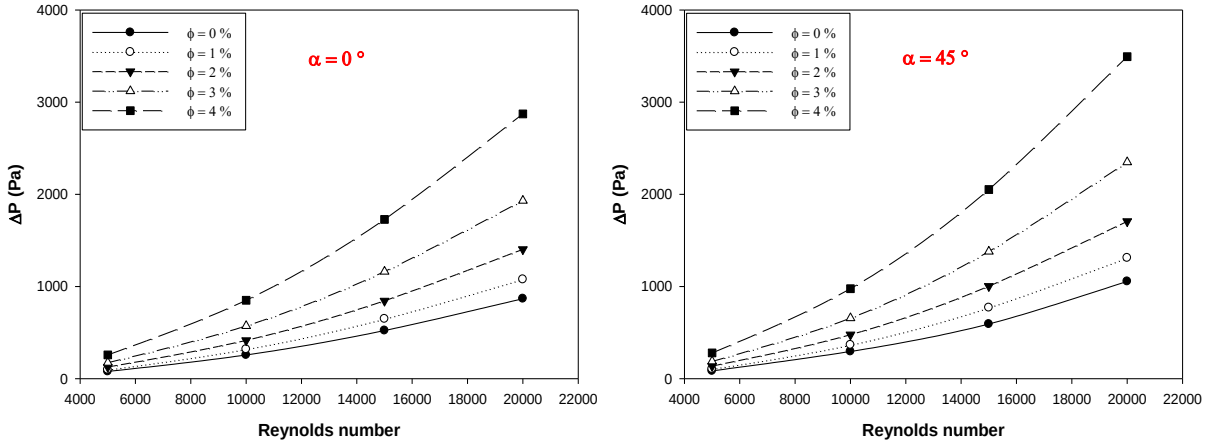

Figure 9 Pressure drop, a) α=0°, b) α = 45°

Conclusion

The fluid flow and heat transfer characteristics of Al_2O_3 nanofluid in triangular corrugated channel was investigated numerically. The governing equations were solved utilizing finite volume method with the SIMPLE algorithm. The effect of nanofluid volume fraction and the corrugation of the upper and lower walls were investigated as function of Reynolds number. The results show that heat transfer increases by increasing the nanofluid volume fraction and the inclination of triangular cavities. The enhancement of heat transfer accompanied with an increase in pressure drop.

Nomenclature

Symbol	Name, *unit*		*Greek symbols*
Cp	specific heat at constant pressure, J/kg.K	α	inclination, degree
Dh	hydraulic diameter, m	β	modeling function
dp	diameter of nanofluid particles, nm	μ	dynamic viscosity of the fluid, Pa s
e	height of triangular corrugation, m	ρ	density of the fluid, kg/m^3
F	friction factor	Φ	volume fraction, %
H	channel height, m	ε	dissipation kinetic energy, m^2/s^3
h	convective heat transfer coefficient, W/m^2 K		
k	thermal conductivity of the fluid, W/m·K		Indices
L	length of channel, m	i	inlet
M	molecular weight of base fluid	o	outlet
N	Avogadro number = 6.022x10^{+23}, mol^{-1}	f	fluid
Nu	Nusselt number	p	particle
ΔP	pressure, Pa	nf	nanofluid
Pr	Prandtl number	np	nanoparticle
P	pitch between two successive	t	turbulent

	corrugations, m		
Re	Reynolds number	w	Wall
T	temperature,K		
w	length of triangular corrugation, m		

Références

[1] Y. He, Y. Mena, Y. Zhao, H. Lu, Y. Ding, Numerical investigation into the convective heat transfer of TiO2 nanofluids flowing through a straight tube under the laminar flow conditions, Applied Thermal Engineering, 29, 1965–1972, 2009

[2] H.A. Mohammed, G. Bhaskaran, N.H. Shuaib, H.I. Abu-Mulaweh, Influence of nanofluids on parallel flow square microchannel heat exchanger performance, International Communication in Heat and Mass Transfer, 38, 1–9, 2011.

[3] Mendes P, Sparrow EM. Periodically converging–diverging tubes and their turbulent heat transfer, pressure drop, fluid flow, and enhancement characteristics, Journal of Heat Transfer; 106, 55–63, 1984.

[4] Sang I, Hyung N. Experimental study on flow and local heat/mass transfer characteristics inside corrugated duct. International Journal of Heat and Fluid Flow, 27, 21–32, 2006.

[5] L. Pingan, G. Ye, M. Hairong, Han Liu, Numerical simulation of heat transfer and resistance pattern in channels with different ribs, International Conference on Computer Design and Applications (ICCDA 2010), 2010.

[6] W. Qu, G.M. Mala, D. Li, Heat transfer for water flow in trapezoidal silicon microchannels, Int. J. Heat Mass Transfer, 43, 3925–3936, 2000.

[7] F. Javadi, S. Sadeghipour, R. Saidur, G. BoroumandJazi, B. Rahmati, M. Elias, M. Sohel, The effects of nanofluid on thermophysical properties and heat transfer characteristics of a plate heat exchanger, Int. Commun. Heat Mass Transfer, 44, 58–63, 2013.

[8] M.B. Turgay, A.G. Yazicioglu, Effect of surface roughness in parallel-plate microchannels on heat transfer, Numerical Heat Transfer, Part A 56, 497–514, 2009.

[9] Y. Xuan, Q. Li, Investigation on convective heat transfer and flow features of nanofluids, Journal of Heat transfer 125 (2003) 151–155.

[10] A.K. Santra, S. Sen, N. Charaborty, Study of heat transfer due to laminar flow of copper–water nanofluid through two isothermally heated parallel plates, International Journal of Thermal Scienc, 48, 391–400, 2009.

[11] A.M. Abed, K. Sopian, H. Mohammed, M. Alghoul, M.H. Ruslan, S. Mat, et al., Enhance heat transfer in the channel with V-shaped wavy lower plate using liquid nanofluids, Case Stud. Therm. Eng. 5, 13–23, 2015.

[12] A. Akbarinia, R. Laur, Investigating the diameter of solid particles effects on a laminar nanofluid flow in a curved tube using a two phase approach, International Journal of Heat and Fluid Flow, 30,706–714, 2009.

[13] A. Raisi, B. Ghasemi, S.M. Aminossadati, A numerical study on the forced convection of laminar nanofluid in a microchannel with both slip and no-slip conditions, Numerical Heat Transfer, Part A 59, 114–129, 2011.

[14] H.A. Mohammed , A.N. Al-Shamani, J.M. Sheriff, Thermal and hydraulic characteristics of turbulent nanofluids flow in a rib–groove channel, International Communications in Heat and Mass Transfer 39 1584–1594, 2012.

[15] Azher M. Abed, M.A. Alghoul, K. Sopian , H.A. Mohammed, Hasan sh. Majdi, Ali Najah Al-Shamani, Design characteristics of corrugated trapezoidal plate heat exchangers using nanofluids, Chemical Engineering and Processing 87, 88–103, 2015.

[16] R.S. Vajjha, D.K. Das, D.P. Kulkarni, Development of new correlations for convective heat transfer and friction factor in turbulent regime for nanofluids, Int. J. Heat Mass Transfer 53,4607–4618, 2010.

[17] S. Eiamsa-ard, P. Promvonge, Thermal characteristics of turbulent rib–grooved channel flows, International Communications in Heat and Mass Transfer 36, 705–711, 2009.